 GLAST LAT SYSTEM SPECIFICATION	Document # <b>LAT-TD-00</b>	Date -January-2006
	Author(s) Lott & do Couto e Silva	
	Subsystem/Office Integration and Test	
Document Title <b>CERN Beam Test Plan</b>		

## **Gamma-ray Large Area Space Telescope (GLAST)**

### **Large Area Telescope (LAT)**

### **Integration & Test Subsystem**

### **CERN Beam Test Plan**

**Change History Log**

Revision	Effective Date	Description of Changes

---

<b>1. Introduction</b> .....	<b>5</b>
<b>1.1. Verification of requirements</b> .....	<b>5</b>
<b>1 Parameter</b> .....	<b>5</b>
<b>1.2. Need for tuning the Monte-Carlo simulations</b> .....	<b>6</b>
<b>2. Definitions</b> .....	<b>7</b>
<b>2.1. Acronyms</b> .....	<b>7</b>
<b>2.2. Definitions</b> .....	<b>7</b>
<b>3. Applicable Documents</b> .....	<b>7</b>
<b>4. Description of the Calibration Unit (CU)</b> .....	<b>8</b>
<b>5. Specific areas where Gleam-GEANT4 is to be tested</b> .....	<b>9</b>
<b>5.1. Point Spread Function (PSF)</b> .....	<b>9</b>
<b>5.2. Effective area</b> .....	<b>10</b>
<b>5.3. Energy reconstruction and absolute energy calibration</b> .....	<b>10</b>
<b>5.4. Backsplash determination</b> .....	<b>11</b>
<b>5.5. Background rejection</b> .....	<b>11</b>
5.5.1. Hadronic reaction patterns .....	11
5.5.2. Positron annihilation .....	12
<b>5.6. GEANT4 Validation</b> .....	<b>12</b>
<b>5.7. Flight electronics response</b> .....	<b>13</b>
<b>5%</b> .....	<b>14</b>
<b>6. Description of Beams and Setups at PS and SPS</b> .....	<b>15</b>
<b>6.1. PS</b> .....	<b>15</b>
<b>6.2. SPS</b> .....	<b>15</b>
<b>7. DAQ systems – Trigger</b> .....	<b>16</b>
<b>8. Description of Monte-Carlo simulations specific to the beam test</b> .....	<b>16</b>
<b>9. Offline infrastructure</b> .....	<b>17</b>
<b>9.1. Digitization</b> .....	<b>17</b>
<b>9.2. Simulation and Reconstruction</b> .....	<b>17</b>
<b>9.3. Code Management</b> .....	<b>17</b>
<b>9.4. Change Control</b> .....	<b>17</b>
<b>9.5. Data Processing</b> .....	<b>17</b>
<b>9.6. Near Real-Time Monitoring</b> .....	<b>18</b>
<b>10. Calibrations</b> .....	<b>18</b>
<b>10.1. Cosmic muon calibrations</b> .....	<b>18</b>
<b>10.2. In-beam calibrations</b> .....	<b>18</b>
<b>11. Configurations-Statistics</b> .....	<b>19</b>
<b>11.1. PS</b> .....	<b>19</b>
11.1.1. Tagged gamma-rays .....	19

---

11.1.2.	Electrons .....	19
11.1.3.	Positrons .....	20
11.1.4.	Hadrons.....	20
11.1.5.	Muons .....	20
11.1.6.	Summary at PS .....	20
<b>11.2.</b>	<b>SPS .....</b>	<b>21</b>
11.2.1.	Electrons .....	21
11.2.2.	Hadrons.....	21
11.2.3.	Summary at SPS .....	21

## 1. Introduction

### 1.1. Verification of requirements

The requirements for the Beam Test program flow down from the LAT Performance Specification – Level II(b) Specification Document (LAT-SS-00010-02). The Beam Test program is designed to ensure that the performance of the LAT meets the requirements of LAT-SS-00010-02. The performance requirements, for which the Beam Test program is relevant, have been summarized in Table 1. This Beam Test plan is required in the LAT Program Instrument Performance Verification Plan (LAT-MD-00408).

*Table 1. Summary of Science Instrument Performance Verification (a subset of Table 1 of LAT-SS-00010-02). A column has be added to the table indicating which beam tests are relevant to verifying the requirement. The verification methods are T=Test., A=Analysis.*

Req't #	Req't Title	Parameter	Verification Method	Beam Tests relevant to the Verification
5.2.1	EnergyRange/ Effective Area	At Normal Incidence: > 300 cm <sup>2</sup> @ 20 MeV >3000 cm <sup>2</sup> @ 100 MeV >6400 cm <sup>2</sup> @ 300 GeV	T=Test A=Analysis  T + A	Brem beam, simultaneously all $\gamma$ energy bins from 50 MeV to 2 GeV, variety of angles and transverse positions.
5.2.2	Energy Resolution	On axis: $\leq 50\%$ 20–100 MeV $\leq 10\%$ .1-10 GeV $\leq 20\%$ 10-300 GeV $\leq 6\%$ >10 GeV, Incidence>60°	T + A	1) Tagged photons 50 MeV to 2 GeV, variety of angles and transverse positions 2) Electrons 0.3,1,5,10,15,20, 50,100,200,300 GeV, (TBD) variety of angles and transverse positions
5.2.3	Peak Effective Area	>8000 cm <sup>2</sup>	T + A	1) Brem beam, simultaneously all $\gamma$ energy bins from 50 MeV to 2 GeV, variety of angles and transverse positions.
5.2.4	Effective Area Knowledge $\Delta A/A, 1\sigma$	<50% 20-50 MeV <25% .05-300 GeV	T + A	1) Brem beam, simultaneously all $\gamma$ energy bins from 50 MeV to 2 GeV, variety of angles and transverse positions.
5.2.5	Single Photon Ang Resolution 68% (on-axis)	< 3.5° front @ 100 MeV < 6° back  < 0.15° front @ 10-300 GeV < 0.3° back	T + A	1) Brem beam, simultaneously all $\gamma$ energy bins from 50 MeV to 2 GeV, variety of angles and transverse positions
5.2.6	Single Photon Ang Resolution 95% (on-axis)	< 3 x $\theta_{68\%}$ On-Axis	T + A	1) Brem beam, simultaneously all $\gamma$ energy bins from 50 MeV to 2 GeV, variety of angles and transverse positions.
5.2.7	Single Photon Ang Resolution (off axis at 55°)	< 1.7 times on-axis	T + A	1) Brem beam, simultaneously all $\gamma$ energy bins from 50 MeV to 2 GeV, variety of angles and transverse positions.
5.2.8	Field of View	> 2 sr	T + A	1) Brem beam, simultaneously all $\gamma$ energy bins from 50 MeV to 2 GeV, variety of angles and transverse positions.
5.2.11	Time Accuracy	Better than 10 usec rel to S/C time	T + A	1) All Beam Test events record time with respect to external GPS
5.2.12	Background Rejection	>10 <sup>5</sup> :1 (TBR)	T + A	1) 1 M protons (Pattern rejection) 2) Cosmic rays on the ground (ACD rejection)
5.2.13	Dead Time	<100 usec per event	T + A	1) Ground cosmic 2) All Beam Test runs

## 1.2. Need for tuning the Monte-Carlo simulations

The Beam Test Rationale (LAT-TD-02152-02) justifies the need for a beam test. Only a few elements are repeated here.

A sophisticated Monte-Carlo model of the instrument, GLEAM, has been developed based on GEANT4. The instrument response functions (IRFs), including effective area, PSF, reconstructed energy distributions, required for analyzing the data will be established with this model. It is indeed not feasible to scan the whole phase space continuously as a function of angles (polar and azimuthal), positions and energies with a gamma-ray beam. However, an extensive set of data sampling this phase space must be collected to verify that the predictions of the simulations match the response of the actual instrument. This data set will serve as a basis for improving the simulations in case of significant discrepancies. Two aspects of the simulations are to be tested: the modeling of basic physical processes like multiple scattering, shower development, ect... on the one hand and the detector modeling on the other hand. As GEANT4 only provides the energy deposited in a given volume, the subsequent steps leading from this energy to the signal actually recorded by the electronics have to be modeled independently. These steps involve quantities that cannot easily be determined *a priori*, but usually result from a calibration process or are assumed from specifications. It is important to verify the accuracy of these quantities as much as possible. Discrepancies between data and simulation results may manifest flaws in the calibration procedures or reveal previously unknown effects, as non-linearity or inefficiency effects for instance. Problems with the description of the geometry may also be revealed.

The good reproduction of both directly-measured parameters (deposited energy, hit multiplicities) and quantities resulting from a high-level analysis (reconstructed energy and direction) must be checked in different regions and particularly at both ends of the LAT energy band, each being important in its own right. Most photons detected by the LAT will have low energy, as typical gamma-ray sources have power-law photon distributions with indices close to -2. On the other hand, the coverage of the energy band 1-300 GeV is of prime scientific importance and constitutes one of the major breakthroughs with respect to EGRET. The extinction of most EGRET sources takes place within this energy band, the precise high-energy cutoffs remaining unknown so far.

The detector will be tilted with respect to the beam axis at angles ranging from 0 to 90 deg. At finite angles, different positions will be scanned corresponding to particles crossing gaps at different “depths” in the tracker or the calorimeter.

The PS will provide:

- electrons, protons or pions, muons from 300 MeV to 15 GeV;
- tagged gamma-rays from 50 MeV (TDB) up to 2 GeV (TBD).

The SPS will provide:

- electrons, protons or pions, from 10 GeV to 300 GeV;

## 2. Definitions

### 2.1. Acronyms

ACD	Anti-Coincidence Detector
CAL	Calorimeter
CU	Calibration Unit
DAQ	Data Acquisition system
EGSE	Electronic Ground Support Equipment
EM	Engineering Model tower.
GEANT4	GEometry And Tracking version 4
GLAST	Gamma-ray Large Area Space Telescope
GLEAM	GLAST LAT Event Analysis Machine
I&T	Integrate and Test
LAT	Large Area Telescope.
MIP	Minimum Ionizing Particle
PS	Proton Synchrotron
SPS	Proton Supersynchrotron
SVAC	Science Verification and Calibration
SSD	Silicon Strip Detector
TAC	Access Time from Clock
TBD	To Be Determined
TBR	To Be Reviewed
TKR	Tracker
TOF	Time Of Flight
TOT	Time Over Threshold
TRD	Transition-Radiation Detector

### 2.2. Definitions

Tracker        Silicon strip tracker within each tower of the LAT

## 3. Applicable Documents

- [1]    LAT-SS-00010        LAT Performance Specification – Level II(b)
- [2]    LAT-MD-03489        Ad Hoc Committee on End-to-End Testing

- 
- |     |                 |  |
|-----|-----------------|--|
| [3] | LAT-MD-00575    | SVAC LAT Plan for LAT Integration at SLAC            |
| [4] | LAT-MD-00408    | LAT Program Instrument Performance Verification Plan |
| [4] | LAT-TD-02152-02 | LAT Beam Test Rationale                              |

#### 4. Description of the Calibration Unit (CU)

The CU will be composed of two spare towers meeting the flight standards plus one additional calorimeter forming a line of 3 adjacent elements. These modules will be integrated into a 1X4 grid similar to a X slice of the LAT flight grid (bays 0,1,2,3), the extra bay being filled with a dummy calorimeter. Using 3 towers in line will allow the effects of inter-tower gaps on the direction and energy reconstructions to be investigated. The whole set of detectors plus the TEM will be enclosed in a sealed container flushed with dry nitrogen. The container will be made of 2mm-thick Al. Five (TBD) ACD tiles will be placed at different positions outside this container for backplash studies. They will be attached in a loose way so that they can be moved at different locations during the experiment. All detector elements will be fitted with flight electronics. The CU will be sitting horizontally on a rotating plate mounted on a X-Y scanning table. This table will thus allow for 3 degrees of freedom: vertical translation, horizontal translation, rotation around the vertical axis.

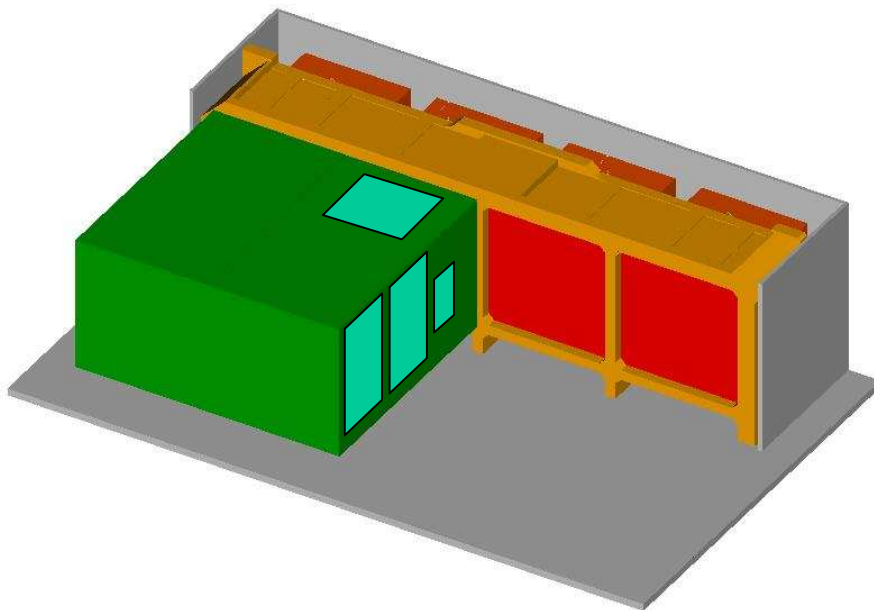


Figure 1. Sketch of the CU. The right-most grid bin is populated with a dummy calorimeter. Some ACD tiles are shown at possible locations.



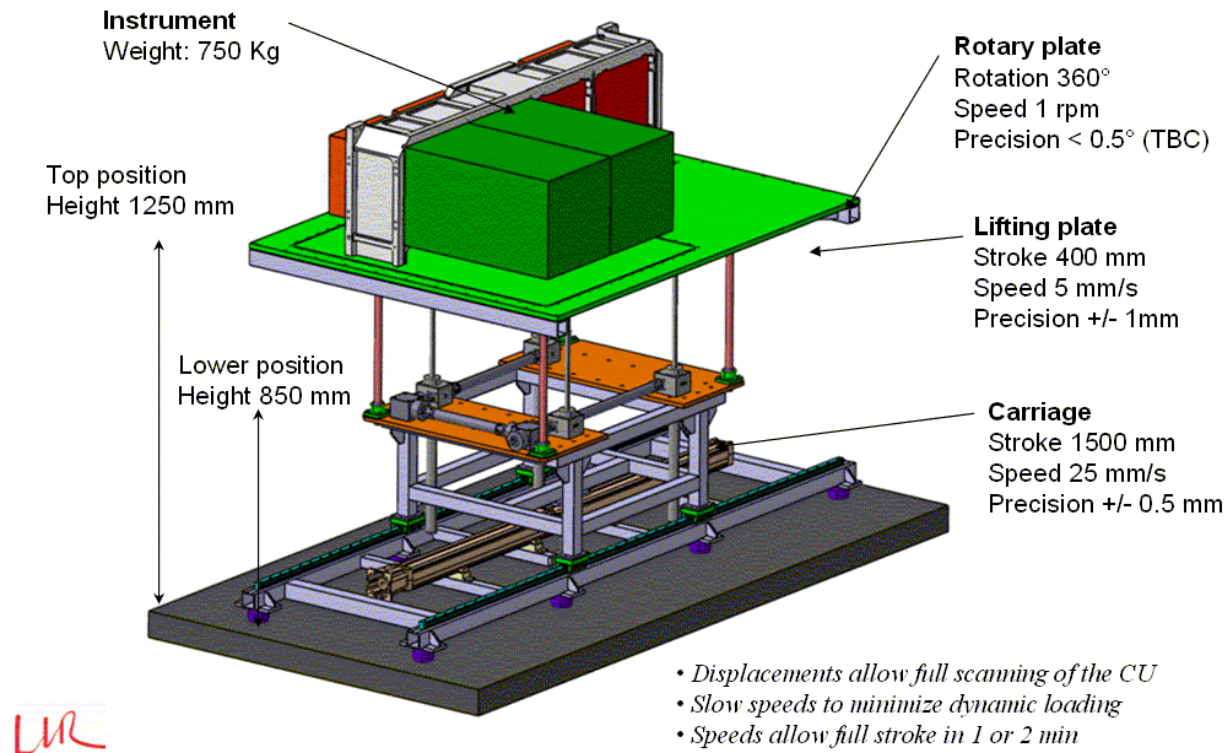


Figure 2. Sketch of the CU on the XY-theta table.

## 5. Specific areas where Gleam-GEANT4 is to be tested

For each configuration/setting, Monte-Carlo simulations will be performed to generate a data set that will be analyzed with the same routines as the real data.

Thereafter are listed specific items requiring verification.

### 5.1. Point Spread Function (PSF)

A precise measurement of the PSF, the LAT key parameter, with low-energy gamma -rays is of paramount importance, in particular to enable the resolution of faint sources in the vicinity of bright ones. For the LAT, multiple-scattering suffered by the primary  $e^+e^-$  pairs (mostly in the W conversion foils) governs the PSF. This physical process is well understood, but it is good to check that the simulated data match the real ones.

A more critical area requiring special attention in the context of the PSF is the production of very soft electromagnetic particles in and around the shower core. The distributions of soft electrons, often referred to as “delta rays” or “knock-on” electrons, depend on the detailed modeling. These particles are important as they both enlarge cluster size for shower core particles as well as create a halo of “noise” hits, which is a source of confusion for the pattern recognition. The energy down to which particles are produced and transported in GEANT 4 is controlled by an effective range cut-off: smaller values result in increased time for simulations while large values run the risk of truncating important effects. The current simulations run with this parameter set to 100  $\mu\text{m}$  for the

Tracker and 700  $\mu\text{m}$  for the other volumes. The size of the clusters recorded by the TKR, as well as the associated TOT distributions, will be the key parameters in this study.

A convenient way to fit the PSF at a given energy is to use the following function introduced by

Toby Burnett (LAT-AM-4355):  $f(u) = \left(1 - \frac{1}{\gamma}\right) \left(1 + \frac{u}{\gamma}\right)^{-\gamma}$  with:  $u = \frac{1}{2} \left(\frac{r}{\sigma}\right)^2$ ,  $r$  being the angular deviation between the true and reconstructed directions divided by an energy-dependent scaling function,  $\sigma$  and  $\gamma$  being the two fitted parameters (see Figure 2).

## 5.2. Effective area

At given incident energy and angle, the effective area is governed by two factors:

- the efficiency of the reconstruction algorithms in providing meaningful outputs, which is hampered if the number of hits recorded by the TKR or the energy measured by the CAL are too low;
- the probability for the gamma-rays of passing the background-rejection cuts. These background cuts are determined via a “classification tree” analysis and optimized to obtain a reasonable trade-off between residual background rate and effective area.

The distributions of the relevant parameters must all be checked carefully using the gamma-ray or proton data at different positions and angles and appropriately tuned if significant discrepancy is observed.

## 5.3. Energy reconstruction and absolute energy calibration

Longitudinal and transverse deposited energy profiles will be measured, as well as total energy distributions. It is worthwhile to note that only very few detailed comparisons between experimental and simulated longitudinal profiles can be found in the literature.

The energy reconstruction is complicated by the large gaps separating the towers. Several effects result from a shower crossing these gaps: the pattern of energy deposited per layer is affected, part of the energy escape through these gaps while direct energy deposition within the photodiodes bordering the gaps leads to an overestimation in the energy deposited within the corresponding crystal.

Different energy-reconstruction algorithms are necessary as the LAT energy band covers 4 decades. In the low end of the band, the algorithm makes use of the information from both the tracker (strip hit multiplicity) and the calorimeter, as a large fraction of the energy is lost in the 1.5  $X_0$ -thick tracker in that case. At higher energy, as the calorimeter is only 8.5  $X_0$ -deep at normal incidence, the energy deposited in the calorimeter represents a small fraction of the initial particle energy (40 % for a 300 GeV on-axis gamma-ray). Three algorithms each giving optimal results in different regions of the (angle, position, energy) phase space have been developed to estimate the energy leakage:

- the “parametric” method;
- the “profile-fitting” method;
- the “tracker + last-layer correlation” method.

The accuracy of the different methods will be tested at PS (with photons and electrons) and SPS (with electrons).

The performance of the algorithm determining the initial direction of the incident particle by using the positions provided by calorimeter will be tested as well. This is specially important for "CAL-only" events where particles enter the calorimeter sideways at a very shallow angle, without traversing the tracker. The energy resolution is improved in that case as the particles encounter a larger calorimeter depth than particles close to the instrument axis, at the expense of a poor direction reconstruction. This event class is of interest for dark matter searches for instance.

#### 5.4. Backsplash determination

For high energy gamma-ray showers, some X-rays escape the calorimeter backward and can fire the ACD, producing a false veto signal. This problem greatly hampered EGRET's acceptance at high energy, severely limiting its energy range. To mitigate this problem, the LAT's ACD is segmented into 89 tiles and it is imposed in the analysis that the incident particle's trajectory does not intersect any firing tile. It is crucial to check that the simulation reproduces the backplash characteristics (incident-energy dependence, angular distribution, pulse-height amplitude distribution, dependence on the distance between tile and impact on CAL). For off-axis showers, the maximum of the effect does not peak at 180 deg. anymore but at a smaller angle where the secondary particles encounter the minimum thickness of material on their way out. For the same reason, the overall deposited energy is greater as some electrons may contribute in addition to photons.

Showers entering the calorimeter close to a gap are most conducive to backplash as X-rays can escape sideways through the gap. The dependence of the backplash amplitude on the distance to the gap must thus be investigated.

#### 5.5. Background rejection

##### 5.5.1. Hadronic reaction patterns

As already pointed out, the rejection of the hadronic background is a crucial issue for the LAT. The corresponding algorithms have been developed thanks to simulations. Benchmarking the hadronic simulations with real data is necessary, all the more as hadronic showers are much more difficult to model accurately than electromagnetic showers. High statistics is required here since the rare hadronic showers having patterns mimicking those of electromagnetic showers are of special interest.

Thereafter is a list of distributions that have been used in past proofs of background rejection as input to the hadron beam test verification requirements. This list is divided into the following logical categories:

- 1) CAL energy distributions:
  - a. topologies and numbers of hit crystals, particularly transverse relative to energy centroids and known event axes
  - b. energy depositions per layer

This is considerably complicated by the gaps and materials between CAL modules. As for the energy reconstruction, understanding the effect of the gaps is key to the background rejection.

- 2) TKR topologies. The key distributions are the track hit distributions at the head of the tracks as well as hit populations about the event axis, both near by as well as outside a given transverse distance.

- 3) TKR-CAL matching. These variables compare the location as well as the direction of the reconstructed event axis from the tracker to that measured in the Calorimeter. At low energy, only the distance for the projected axis to the energy centroid has merit, however at high energy the Calorimeter provides an independent direction for the event axis.
- 4) Low Energy Particle Range-outs: Both the Z location of where tracks start and stop as well as the TOT from the tracker.

The last two cases pertain to situations where a side-incident proton in the calorimeter produces a hadronic shower with one or several low-energy protons flying into the tracker and stopping within, mimicking a converting downgoing gamma-ray.

The basic goal of the beam test will be to compare the distributions of these variable classes with those found experimentally.

Protons will be used whenever possible, but at high energy, the available rate may be too low. In that case, we will use  $\pi$  instead as  $\pi^-$  and proton-induced reactions are essentially indistinguishable at energies beyond 5 GeV (the validity of this statement will be checked at a given energy, where both proton and pion rates are high).

The performance of the “MIP finder” algorithm, developed to identify proton events through the presence of a deposited-energy pattern in the calorimeter consistent with that expected for such particle until it undergoes a hadronic interaction, will be tested as well.

### 5.5.2. Positron annihilation

Gamma-rays produced by positron annihilation in the micrometeorite shield and thermal blanket constitute a major part of the irreducible background. At PS, the lower energy available for a positron beam is about 1 GeV (TBD), at which the annihilation cross-section is only about 1 barn, corresponding to a probability for a positron to annihilate within the outer material of about  $10^{-4}$ . Both the annihilation probability and the detection pattern of the gamma-rays will be investigated at CERN. As the probability for both annihilation gamma-rays to leave a signal in the detector is fairly high, methods can potentially be developed to discriminate these two-photon events.

An important issue concerns the estimation of the positron flux in orbit, so that precise correction for the residual background can be made. In orbit, background runs (i.e. with the ACD disabled) will be performed. Signature for annihilation within the tracker allowing positrons to be told apart from electrons can be sought for. The corresponding methods will be tested with the CERN data.

## 5.6. GEANT4 Validation

The verification process underlined above will also enable the modeling of physics processes in GEANT4 to be checked at the same time. This will provide a feedback to the GEANT4 collaboration and enable improvements if significant deficiencies are found. Of particular interest is the modeling of:

- multiple scattering for electrons;
- hadronic interactions;
- electromagnetic showers.

### 5.7. Flight electronics response

The Monte-Carlo simulation takes into account known caveats of the electronics, as the limited size of the tracker FIFO register or non-linearities revealed via charge injection. Running under different conditions in the rate and/or amplitudes of the signals will enable the correctness of this modeling to be verified.

The high counting-rate behavior of the flight electronics (dead time, readout timing adjustment "TAC") will be checked with particle intensities beyond 10000 p/s. Proper synchronization with other DAQs (which have longer dead times) will be hard to maintain at these rates. Runs with the CU triggered internally or externally will be performed.

In orbit, different trigger types are foreseen, the main ones being based either on the information from the tracker ("3 Si planes hit in a row") or the calorimeter("CAL-low" and "CAL-high", with thresholds on individual CsI crystals of ~100 MeV (FLE) and 1 GeV (FHE), respectively). The efficiency of these triggers will be checked as a function of the counting rate.

An effect observed in previous beam tests needs to be investigated with the CU as well: the so-called "fish-eye" effect, corresponding to a bias in the reconstructed angle with respect to the LAT axis towards lower angles. This effect arises from tracks scattering to smaller angles triggering more efficiently than those scattering at large angles and is more prominent for large angles and at low energy.

In cosmic-muon runs with the LAT, the pedestal amplitudes in CAL channels (measured using a random trigger) have been observed to be different from normal if the event occurs within a short time after a high-amplitude event, manifesting a baseline restoration time greater than the 26.5  $\mu$ s dead time. This effect will be studied both at PS and SPS with electrons in dedicated runs, where for each real event (i.e. associated with a particle in the detector), an artificial trigger will be generated after a short, variable delay (from 27 to 300  $\mu$ s for instance) from the first event. This method will enable this effect to be mapped out as a function of time in an efficient way.

The conditions will not be the same as in orbit where the flux will be distributed over the whole instrument area, but these data will nevertheless provide very useful information regarding the instrument response.

<b>ITEM</b>	<b>Distributions</b>	<b>Beam configuration</b>	<b>Target Precision</b>
TKR cluster sizes	TKR cluster sizes by layer	Electrons (few GeV) and/or tagged gammas (100 MeV, 1 GeV) at normal incidence and off-axis	1%
TKR pulse durations	TOT by layer	Electrons (few GeV) and tagged photons (100 MeV, 1 GeV) at normal incidence and off-axis	5%
CAL nuclear counter effect (direct energy deposition in diodes)	Energy centroid position relative to true particle impact position	Electrons (few GeV or higher) at normal incidence and off axis	10%
CAL energy topologies	#hit xtals relative to energy centroid and track axis; energy deposition per layer.	Electrons(100 MeV, few GeV, >10 GeV) or tagged gammas(100 MeV, 1 GeV.); side-incident and normal-incident protons	5%
TKR track topologies	Hit distributions at the track vertex; distributions of hits around tracks (inside and outside "roads")	Tagged gammas (100 MeV, 1 GeV); at normal incidence and off-axis; protons at normal incidence and off-axis	1%
TKR-CAL matching	Difference of track projection and CAL energy centroid	Electrons (100 MeV, few GeV) or tagged gammas (100 MeV, 1 GeV) at normal incidence and off-axis; side-incident protons	2%
Low energy particle range-outs	Z location of track starts and stops, # tracks, TOT for stubs; fraction of L1Ts produced.	Side-incident protons.	2%
Backsplash	Energy deposition in tiles at selected positions	Tagged gammas and electrons at different angles	2%
GEANT4 benchmarking (multiple scattering, EM showers, hadronic showers)	All hit and deposited energy distributions	All the above	2%
PSF	PSF distribution and 68% and 95% containment values	Tagged gammas at normal incidence and off-axis	1%
Systematic photon reconstruction effects (offsets, efficiencies)	Mean reconstructed direction; number of reconstructed photon events compared with tagged rates.	Tagged gammas at 100 MeV and 1 GeV, at normal incidence and off-axis	5% on efficiencies
Photon energy reconstruction	Reconstructed energy distributions	Tagged gammas at 100 MeV<E<1GeV, normal incidence and off-axis, at a few incident positions to explore gaps. Electrons at a few GeV and at >100 GeV effective at normal incidence and off-axis, at a few incident positions to explore gaps.	5%

Table 2. Summary of information from beam test. The upper part consists of direct component comparisons while the lower part lists end-to-end tests.

## 6. Description of Beams and Setups at PS and SPS

### 6.1. PS

The gamma-tagging setup developed for testing the AGILE tracker in T9 will be used (Fig to be added). A plastic detector, about 2 cm x 2 cm (TBD) in dimension will provide the trigger signal for the different DAQ. Bremsstrahlung photons will be produced in silicon detectors measuring the position of the incident electrons, referred to as silicon chambers in the following. The beam momentum bite will be limited to 1% by opening the corresponding slits to 3 mm (TBD). The total thickness of these detectors will be 1.6 mm (TBD), corresponding to 0.017 radiation length. This low thickness is desirable as it limits the probability of having more than one gamma-ray per event. After crossing these detectors, the electrons will be deflected by a magnet with a field of about 1 T, and their deflection angle will be measured with a precision of 5 mrad, corresponding to a momentum precision of 2.5%. Different electron energies will be required to cover the energy range 50 MeV-2 GeV with a reasonable accuracy, the gamma-ray energy being determined as the difference between the electron initial and final energies. To first approximation, the bremsstrahlung spectrum has equal numbers of  $\gamma$ -rays per percent width energy bin.

In the AGILE experiment, about 100 gamma-rays per 400 ms-long spill were recorded. A similar rate is expected for the LAT experiment. During the calibration procedure, the beam will be deflected to an angle corresponding to the center of the strip detector. Then the magnetic field will be reduced or the detector translated away from the beam axis together with the downstream plastic detector so as not to intercept the unradiated electrons. The dead time of the DAQ reading out the four silicon chambers' information is 500  $\mu$ s due to multiplexing, so triggering on the direct beam while keeping a reasonable gamma-ray rate would lead to a large dead-time. However, the position distribution of electrons associated to gamma-rays with energy lower than 100 MeV will strongly overlap with that of the unradiated electrons, and for the specific runs dedicated to low-energy gamma-rays, there will be no choice but to trigger on the unradiated beam as well. For 50% dead time and 10% of the electrons being associated with a gamma-ray with  $E > 20$  MeV, the rate of these gamma-rays will only be 40 per spill.

For orientation, at 1 GeV, the beam composition in T9 measured via TOF is 7% p, 73% e and 20%  $\pi$ . The particle ID will be performed by a combination of TOF (TBD), TRD and Cherenkov-counters.

Runs with electrons will also be performed to ensure proper overlap with the SPS data.

### 6.2. SPS

The high-precision H4 beam line will be used. It provides the highest electron energy, 300 GeV corresponding to the high-end of the domain covered by the LAT, with low hadron contamination (lower than 1% beyond 50 GeV). The discrimination between electrons and hadrons will be performed thanks to a transition-radiation detector (TRD). At low energy ( $E \sim 20$  GeV), two Cherenkov counters will be used.

A set of plastic detectors will also be placed upstream to provide the trigger signal and veto off-axis particles.

## **7. DAQ systems – Trigger**

The success of the experiments crucially depends on a proper synchronization of the different DAQs recording the information from either the CU or the ancillary detectors. To this end, the CU will be triggered externally with a signal provided by a set of plastic scintillator detectors located in the beam. The rate will greatly depend on the running conditions. In the gamma-tagging mode, the bottleneck will come from the readout of the ancillary silicon detectors used to define the electron trajectory, which induces a dead time of 500  $\mu$ s per event.

The DAQ for the CU will be the existing LATTE 4.

The ancillary detectors (AD) will all be read by a custom DAQ that combines several ADCs for readout of the scintillators, the Cerenkov and the TRD (a set of 16 stations of 32 straw tubes each), multiplexed ADC for the silicon detector readout, I/O registers, sequencer board for control signals, custom trigger and spill board, and a VME controller interfaced to a PC. The AD DAQ outputs data in root format. Differently from the LAT, where each single event is processed after the other, exploiting buffers in the hardware and multi-threaded acquisition software, the AD DAQ events are buffered in memory and block-transferred to disk. This is due to the fact that the LAT DAQ must take data continuously, while the AD DAQ was conceived to maximize data flow in a spilled beam environment, and therefore uses the off-spill time for time-consuming tasks like data transfer to disk. The AD DAQ was developed and is maintained by INFN-Bari, where the system has been used for a very long time with cosmic rays (CR) and for many CERN beam tests in the past.

The current baseline for merging the data streams is to add the AD data to the main CU LDF data file, thus creating a new LDF file with all data available for downstream processing. It should be stressed that given the LAT modularity, the LDF format was designed from the beginning for easy additions of extra contributions, provided a proper header is available in the data stream, as is easily constructed for the AD binary output data.

Data merging will first happen on files, i.e. offline, and eventually will be taken care of by a process that will run continuously during data taking and will do the merge between beam spills.

The necessary steps/milestones are:

Create an event builder for merging the data: will create the complete LDF starting from the CU LDF file and the AD binary file. As a consequence, it will be possible to modify Gleam so that it can also perform AD recon on the CU data.

Event builder modification: data streams will be provided by network sockets, rather than by file; such modification is backward compatible, i.e. data merge can always be performed offline from files.

Milestone 1 is considered a straightforward extension to the existing software. On the other hand the impact on data analysis is crucial, as all processing will happen in the SLAC pipeline and a single, complete data file will eventually be available for the users.

Milestone 2 is the final goal of the merge strategy and will happen if resources are available. After milestone 2 most of the analysis of beam test data can be done online and real-time, with immediate feedback on the quality of the data taken.

## **8. Description of Monte-Carlo simulations specific to the beam test**



Dedicated GEANT4 Monte Carlo simulations must include the whole spectrometer at PS and the ancillary detectors at SPS, and generate event file including the properties of the particles susceptible to hit the CU. These files are then used as input for the regular GLAST Monte-Carlo code Gleam. The latter has been modified to be able to cope with several “primary” particles entering the CU simultaneously, which is the case if two or more bremsstrahlung photons are produced in the radiator or in the air, or if other secondary particles subsequently created by the primary electron in the dump for example can reach the CU.

## **9. Offline infrastructure**

### **9.1. Digitization**

LDF files will be produced by LATTE and digitized to Root digis. It is expected that the beamline ancillary data will be included in the LDF format. Gleam will be augmented to digitize the ancillary data.

### **9.2. Simulation and Reconstruction**

CU event reconstruction is performed using the standard Gleam tools. Customization is supplied for the CU geometry. The beam ancillary digitizations will be reconstructed, applying time-dependent calibrations.

Local mirrors of the calibrations files and metadata database will be maintained.

Simulation is done by using a standalone GEANT4 simulation of the beam and beamline, producing an output Root file with particles incident on the CU. This file is the standard MC form that Gleam expects.

### **9.3. Code Management**

A "checkout package", BeamtestRelease, has been defined to manage the beamtest customization of the GlastRelease code base. This defines the package versions for Gaudi-based code as well as the standalone G4 simulation code.

### **9.4. Change Control**

A change control board will be instituted to control changes in code used in the processing pipeline and in near real time monitoring at CERN. It will function in the same way as the I&T-SAS CCB has for LAT integration.

### **9.5. Data Processing**

LDF data will be swept from CERN to the SLAC pipeline for processing. The FastCopy file transfer tool will be used for the sweep, just as it is now for I&T. Turn-around time for processing will be best-effort for available CPU time in the SLAC batch farm. Current estimates for needed disk space are about 30 TB.

Data access will be provided via the LAT Dataserver and the eLog query system.

## 9.6. Near Real-Time Monitoring

A stripped-down version of Gleam will be provided locally to digitize the LDF files and do minimal reconstruction (clustering in the TKR and engineering unit conversion for all subsystems). This can either be run by reading multicast events from LATTE (requires some development effort) or after runs are completed. The FRED event display can be used locally for visualization. We are investigating a minimal full-recon version for running locally as well.

## 10. Calibrations

### 10.1. Cosmic muon calibrations

The CU (Tracker, calorimeter, and tiles) will be calibrated following the similar methods as for the LAT.

### 10.2. In-beam calibrations

Before the experiment, the energy calibrations of the tracker, ACD tiles and calorimeter will be performed with cosmic muons, the calibration coefficients (MeV/ADC) being determined by adjusting the measured deposited-energy distributions to those calculated by Monte-Carlo simulations. For the calorimeter, this procedure enables only the calibration coefficients for the LEX8 range to be determined accurately. Electrons of the highest possible energy will be used to scan the three calorimeters. A scan of 12 points per calorimeter forming a cross pattern is necessary (6 points in the vertical direction, 6 points in the horizontal direction, the beam axis passing at midpoint between two adjacent crystals so as to expose both of them at the same time, Fig.1 left). Cross-calibration between different energy ranges for the same crystal will be performed by comparing the data measured in the overlapping regions (about 600 ADC channels - out of 4095 - for the upper range) of adjacent ranges. Multiplying the LEX8 calibration coefficients by the thus obtained relative factors will provide successively the calibration coefficients for the three upper ranges LEX1, HEX8 and HEX1.

An alternative method, which will be tested with the CERN data, consists in adjusting the calibration coefficients so as to minimize the width of the total-energy distribution measured by the CAL.

A scan (one point every 2 cm, see Fig. 1 right) along the main direction of two crystals will be performed to enable the comparison of the so-obtained tapering curves with those measured with cosmic muons.

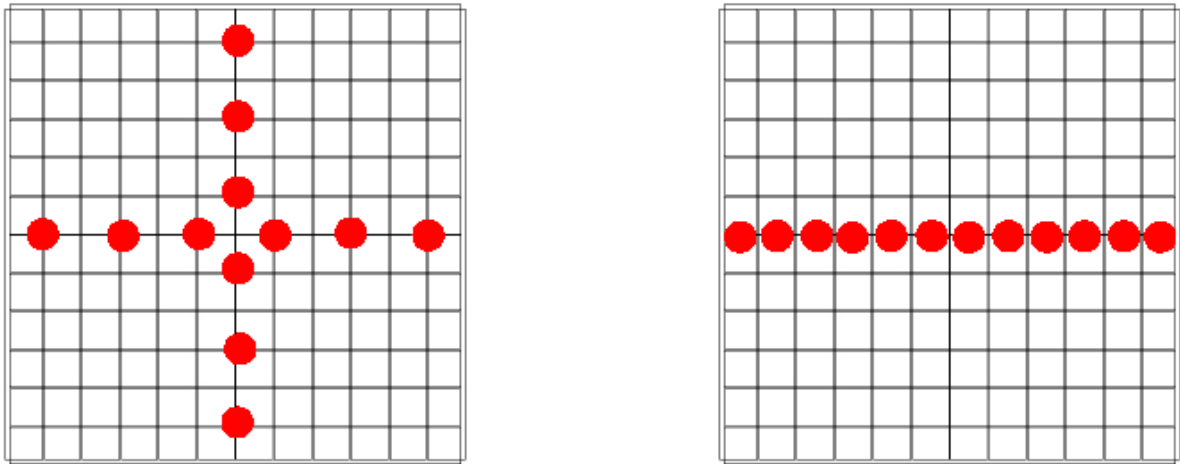


Figure. 1 Left: Positions of beam hits for energy calibration. Right: Positions of beam hits for the determination of the attenuation curve.

Simple science requirements, such as time accuracy and dead time, will also be demonstrated directly from the experimental data.

## 11. Configurations-Statistics

*Note: the effect of beam contamination is to be investigated.*

### 11.1. PS

#### 11.1.1. Tagged gamma-rays

Because of the limited energy resolutions of the tagger and beam dispersion, different beam energies need to be used. Different electron energies: 0.5, 1, 2, 3 GeV (TBD) must be employed to cover the full gamma-ray energy range.

A conservative photon rate of 100 per 400 ms spill, similar to that obtained with AGILE is assumed. Most measurements will be performed at 5 angles (0, 5, 20, 40, 60 deg) and 6 positions allowing the effects of gaps to be investigated. Accumulating 100k events per geometrical setting will necessitate 2 hours of beam time (assuming 2 spill per 17 s- long master cycle).

It must be stressed that in the past beam tuning proved very problematic in the AGILE experiments using the same tagging setup. A total of 2 days are estimated to be necessary for tuning so as to obtain the proper conditions regarding the beam quality, as well for calibrating the spectrometer.

#### 11.1.2. Electrons

The same (angle, position) configurations will be investigated with electrons with energy of 1 GeV, 5 GeV, 10 GeV. A statistics of 200k events per configuration will be accumulated. At 1 GeV, the effect of “upward” electrons will be investigated using two positions at an angle close to 180 deg. The systematic energy calibration described above will be performed at 10 GeV.

**11.1.3. Positrons**

A 1-GeV (possibly 500 MeV) positron beam will be used to study annihilation events. A statistics of at least  $2 \cdot 10^6$  events, corresponding to about 200 annihilation events is needed.

**11.1.4. Hadrons**

Two configurations at 3 energies: 1 GeV, 5 GeV, 10 GeV, will be used: on-axis and side-incident. High statistics is needed: 1 million events per run.

**11.1.5. Muons**

The low-energy calorimeter calibration established with cosmic muons will be checked using mono-energetic (4 GeV), on-axis muons. At GSI, the calibration with on-axis 1.7 GeV protons revealed a 4% discrepancy with that obtained with cosmic muons. On axis particles, six positions,  $10^5$  events will be sufficient. However, the beam rate can be rather low. One assumes 100 Hz.

**11.1.6. Summary at PS**

Particle	Energy (GeV)	Angles (deg.)	#Pos. per angle	Statistics (Time)	Trigger	Configuration
tagged $\gamma$ -rays	0.5,1,2,3 (inc. $e^-$ )	0,5,20,40,60	6	100 k (2 h, tot:10d)	Ext.	4-range
electrons	1,5,10	0,5,20,40,60	6	200k (1h, tot:3.5 d)	Ext.	Flight
	1,5,10	90,180	2	200k (1h, tot:0.5d)	Ext.	Flight
	10	0	60	40k (20 min, tot:1d)	Ext.	4-range
	10	0	1	1M (5h, tot: 2 d)	Int. (high rate)	Several
positrons	1	0	1	2 M (10h, tot: 0.5d)	Ext.	Flight
hadrons	1,5,10	0,90	2+1	1 M (5h, tot:3 d)	Ext.	Flight
muons	4	0	6	100 k (5h, 1d)	Int.+Ext.	Flight

**11.2. SPS**

Running at 500 Hz during the 5 s-long spill (one per 32 s) and assuming a 60% overall duty factor, 200 k events will be accumulated in one hour. Except at the highest energy, and possibly at the lowest, the beam rate should be largely greater.

**11.2.1. Electrons**

For energy reconstruction: 4 angles (0, 20, 40, 60 deg), 5 positions at 6 energies (10, 20, 50, 100, 200, 300 GeV), 200k events per configuration.

For CAL-only events: 90 deg., 2 positions, 200k events at 2 energies.

For backsplash studies: (in addition to above) 3 positions close to a gap, 200k events at two energies.

One additional days with electrons at 200 GeV will be used to test the flight electronics under various conditions. It is best to do this study at high energy with rates up to  $10^4$  Hz.

**11.2.2. Hadrons**

Two configurations, on-axis and side-incident will be used.

High statistics is needed: 1 M events per run. 4 energies: (10, 20, 50, 100 GeV)

**11.2.3. Summary at SPS**

<b>Particle</b>	<b>Energy (GeV)</b>	<b>Angles (deg.)</b>	<b>#Positions per angle</b>	<b>Statistics (Time)</b>	<b>Trigger</b>	<b>Configuration</b>
<b>Electrons</b>	10, 20, 50, 100, 200, 300	0, 20, 40, 60	5	200k (1h,tot:5d)	Ext.	Flight
	20-200	0, 20, 40, 60	3	200k (1h,tot:1d)	Ext.	Flight
	200	0	1	200k(1h,tot:1d)	Int.	Several
	50, 200	90	2	200k(1h,tot:8h)	Ext.	Flight
	10, 20, 50, 100, 200, 300	180	2	200k(1h,0.5d)	Ext.	Flight
<b>hadrons</b>	10,20,50,100	0, 90	2	1 M (5h,3d)	Ext.	Flight

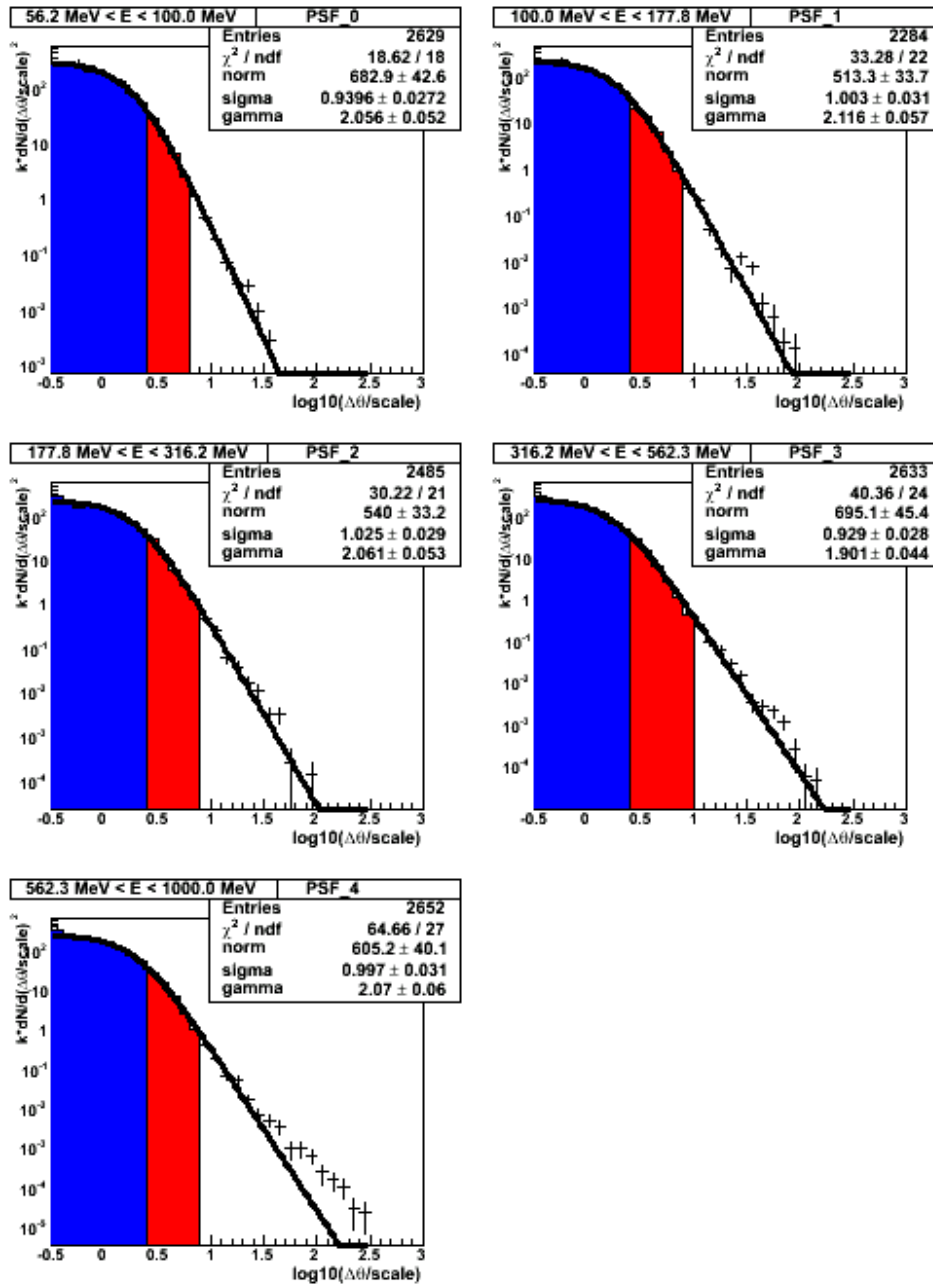


Figure 2. Distributions of the angular difference between reconstructed and true direction of the incident photon, normalized with an energy-dependent scaling parameter, as established from Monte-Carlo simulations